

Published in final edited form as:

Inorg Chem. 2011 February 21; 50(4): 1176–1183. doi:10.1021/ic1020274.

Linear Correlation between ^1H and ^{13}C Chemical Shifts of Ferriheme Proteins and Model Ferrihemes

Fei Yang, Tatiana K. Shokhireva, and F. Ann Walker

Department of Chemistry and Biochemistry, The University of Arizona, PO Box 210041, Tucson, AZ 85721-0041

Abstract

The $^1\text{H}\{^{13}\text{C}\}$ -HMQC experiment at natural abundance ^{13}C provides a very useful way of determining not only proton, but also ^{13}C chemical shifts of most heme substituents, without isotopic labeling of the heme. This is true both in model low-spin ferriheme complexes and in low-spin ferriheme proteins, even when the proton resonances are buried in the protein diamagnetic region, because the carbon shifts are much larger than the proton shifts. In addition, in many cases the protohemin methyl cross peaks are fairly linearly related to each other, with the slope of the correlation, $\delta^{\text{C}}/\delta^{\text{H}}$, being approximately -2.0 for most low-spin ferriheme proteins. The reasons why this should be the case, and when it is not, are discussed.

Introduction

In 1973, Wüthrich and Baumann published the first paper on ^{13}C NMR spectra of several metallocporphyrins (low-spin Fe(III) and Zn(II)) at natural abundance.¹ They used a Varian XL-100 in the pulsed mode for the ^{13}C spectra, and acquired 20,000 transients for Fourier transformation. The signal-to-noise ratio was excellent---on the order of 50:1---for 20 mM samples in 12 mm O.D. NMR tubes. CDCl_3 was used as solvent for the Zn(II)TPP and –Proto(IX) complexes, and 4:1 pyridine- d_5 : D_2O for the Fe(III)TPP and –Proto(IX) complexes, with an excess of KCN present to form the dicyanoiron(III) porphyrin complexes. In 1978 and 1983²³ Goff reported direct-detect spectra of high-spin Fe(III) porphyrins, and in 1981 he reported a detailed study of the bis-imidazole complexes of several tetraphenylporphyrinato-iron(III) complexes.⁴ ^{13}C natural abundance direct-detect experiments have not changed that much since those days, although the availability of the instruments with which to detect them, and the magnetic fields at which they can be carried out has changed a lot. What has also changed dramatically is the ease of ^{13}C enrichment, so that many more researchers are using ^{13}C -enriched starting materials to synthesize complexes that they wish to study, including all possible isotopic enrichments of the last committed precursor to heme synthesis, δ -aminolevulinic acid (ALA).^{5,6} Some of the specifically enriched isomers of ALA have been available from Cambridge Isotopes at various times, but methods for synthesis of the ^{13}C labeled isomers of δ -aminolevulinic acid that are not available commercially have also been developed.⁷ Thus specifically ^{13}C -labeled hemes can be synthesized and used for NMR investigations. Specific $^1\text{H}/^{13}\text{C}/^{13}\text{C}$ experiments have been developed,^{8,9} and used to completely assign the ^{13}C heme resonances of rat outer mitochondrial membrane (OM) cytochrome b_5 ¹⁰ and to learn detailed information about heme electronic structure by studying specifically labeled heme isomers.^{11–15}

In spite of these developments, many scientists still prefer to use nonenriched samples for investigating the ^{13}C resonances of various compounds, including hemes. The $^1\text{H}\{^{13}\text{C}\}$ -HMQC experiment at natural abundance of ^{13}C (1.1%) is an available method that can be used by any researcher who has access to an inverse heteronuclear broadband or ^{13}C (^1H detect) probe. For paramagnetic model hemes and other macrocycles, or heme proteins, this experiment allows correlation of the ^{13}C and ^1H chemical shifts of heme substituents. We and others have found these spectra to be very helpful in identifying and confirming the ^1H chemical shifts of heme and nearby protein substituents whose resonances may or may not be resolved outside the protein resonance envelope.^{16–35} The first people to report a heteronuclear 2D spectrum of a low-spin ferriheme protein, in 1986, were Santos and Turner,¹⁶ in that case a HETCOR. Timkovich was the first to do the inverse experiment, HMQC, on *Ps. aeruginosa* cytochrome *c*-551, in 1991.²⁴ Banci et al. also used the HMQC experiment early to determine the ^1H , ^{13}C shifts of protohemin bis-imidazole and metMbCN in 1994.²⁵ Turner has used this method for aiding the assignment of heme protein resonances since 1995^{16–23} and it is particularly useful for the bis-histidine-bound tetraheme cytochromes *c*₃,^{16,21,23} as shown in Figure 1. It has also been used to investigate model hemes such as the unsymmetrically pyrrole-substituted complex $[\text{2-CITPPFe}(\text{CN})_2]^{-36}$ shown in Figure 2, and the unsymmetrically phenyl-substituted complex $[(o\text{-CONMe}_2)_1\text{TPPFe}(\text{NMeIm})_2]^+$ shown in Figure 3, and other paramagnetic metal macrocyclic complexes such as the chloroiron(III) corrolate π -radicals, for example, $[\text{ClFe}^{\text{III}}(\text{Corr}^{2-\bullet})]$, which are neutrally-charged species with $S = 1$ and large chemical shifts, but short electron spin relaxation times,³⁷ as shown in Figure 4. However, it is worth noting that this is the only complex with $S > \frac{1}{2}$ of which we know, for which the ^1H and ^{13}C spin-lattice relaxation times (T_1 s) are long enough to allow the ^1H , ^{13}C cross peaks to be observed.

We have reported the natural-abundance $^1\text{H}\{^{13}\text{C}\}$ -HMQC spectra of low-spin complexes of the nitrophorin proteins since 2003.^{29–35} By using the information obtained from these HMQC spectra we have been able to assign most of the heme substituent resonances of these protein complexes. For example, in Figure 5 the $^1\text{H}\{^{13}\text{C}\}$ -HMQC spectra of NP2(V24E)-ImH at pH* 7.0, the ^1H , ^{13}C cross peaks of all heme substituents except for those of the *meso*-CH are clearly observed for the **A** heme isomer, and are fairly easy to assign using these $^1\text{H}\{^{13}\text{C}\}$ -HMQC spectra in combination with ^1H , ^1H -NOESY spectra. For the **B** heme isomer, the heme methyl ^1H , ^{13}C cross peaks, except for those of 5M and 8M and the 2- and 4-V α (which are broad because of chemical exchange processes) are also observed. [Note: For those readers unfamiliar with the two possible heme orientations, **A** and **B**, protohemin has no 2-fold rotation axes through the atoms of the heme plane, and thus when it binds to a protein, which is always asymmetric in its structure, two isomers are created. One of these has the heme substituents numbered 1–8 in a clockwise direction if viewed from above the heme plane (assuming the protein-provided ligand is bound below the plane), and the other has the heme substituents numbered 1–8 in a counterclockwise direction if viewed in the same way, as shown in the inserts of Figures 5 and 6. The heme substituents 1–8 will thus be in different environments (have different protein residues near them) for each of these two isomers, and there will thus be two proton (and carbon) resonances for each substituent. Seldom are *all* of these resonances observed, but usually *most* of them are observed.] This particular NP2 mutant is one of the few which has a major **A** orientation of the heme; more commonly it is the **B** heme orientation which is most abundant for NP2, and for which most of the heme resonances are resolved. It is also frequently the rule that the ^1H , ^{13}C cross peak for the most hyperfine-shifted methyl resonance is not observed because of chemical exchange processes;³⁸ in fact, the only pH at which the 3M resonance of the **A** heme orientation for any NP2-ImH complex is observed is pH 7.0 for this V24E mutant shown in Figure 5.

β -Vinyl and α - and β -propionate C-H cross peaks can be spotted because pairs of protons have cross peaks to the same carbon. Examples are the 6- and 7- α -CH₂ propionate cross peaks for the **A** heme isomer of Figure 5, with ¹³C chemical shift -23.9, ¹H chemical shifts +9.0 and +4.2 ppm and ¹³C chemical shift -36.1 ppm, ¹H chemical shifts +12.2 and +12.1 ppm, respectively, for the **A** heme orientation of Figure 5. The corresponding β -CH₂ resonances are at +100.0, -2.2, -2.5 ppm and +125.6, -0.8, -1.6 ppm, respectively, for the **A** heme orientation. (¹H resonance assignments of the 6- and 7 α and β propionate resonances and the 2- and 4 α and - β vinyls are easily confirmed by their NOESY cross peaks.) Other CH₂ groups that are easily recognized are those of His57 β -CH₂, ¹³C chemical shift +20.2 ppm, ¹H chemical shifts +12.7 and +6.3 ppm for the **A** heme orientation, and ¹³C chemical shift +18.6 ppm, ¹H chemical shifts +12.3 and +6.2 ppm for the **B** heme orientation. The His α -CH resonances are very closely spaced at ¹H, ¹³C shifts of 8.3, 69.1 and 8.2, 68.8 ppm. Additional ¹H, ¹³C cross peaks from protein methyls of I120 and L132, which are very close to the heme, are also seen, with ¹³C chemical shifts of 14–16 ppm and ¹H chemical shifts of -1.7 to -2.3 ppm, as will be discussed in further detail elsewhere (Shokhireva, T. K.; Yang, F.; Walker, F. A., in preparation). For wild-type NP2-CN the ¹H, ¹³C cross peaks for all heme substituents except the *meso*-CH are observed, as shown in Figure 6. His57 β -CH₂ cross peaks are also not seen.

To observe these ¹H, ¹³C cross peaks in the HMQC spectrum of a low-spin Fe(III) heme protein requires at least a 1 mM concentration (2 mM is preferable) of ferriheme protein at ¹³C natural abundance, and requires an approximate 24-hour experiment time. Any modern NMR spectrometer equipped with an inverse (¹H observe) ¹³C or broadband probe can be used, and 500 MHz as the ¹H Larmor frequency is certainly sufficient for all systems that have been reported thus far; all of the ¹H{¹³C}-HMQC spectra presented in the author's group's papers have been recorded at 500 MHz.^{29–35} Since inverse ¹³C or inverse broadband probes are common on modern spectrometers, the use of this experiment is strongly recommended to find the heme ¹H resonances which are obscured by the protein resonances, and to then look for these resonances in the WEFT-NOESY spectra of the proteins, to permit complete assignment of the heme resonances. Protein side chains that are close to the heme iron, especially the histidine ligand β -CH₂ and α -CH cross peaks, as well as methyl-, methylene- and aromatic-containing side chains of amino acids that are within ~4 Å of Fe also have unusual ¹H, ¹³C chemical shifts because of the pseudocontact interaction (see below), and can then be followed in the NOESY spectra to assign the side chains of those amino acids.

As shown in Figures 1 and 3 – 6 above, and even more so in Figures 7 and 8 below, which have been created from ¹H and ¹³C data of ¹³C-enriched heme proteins published by Rivera and coworkers^{10–15} and others who have used the ¹H{¹³C}-HMQC experiment on non-enriched heme proteins,^{24–28} the β -pyrrole CH₃ ¹H-¹³C cross peaks of ferriheme proteins usually present a fairly linear correlation of ¹³C and ¹H chemical shifts, with the exception being the case of the pyrrole-H,C resonances of the TPPFe(III) low-spin complex shown in Figure 2.

The unique shifts and the linear correlations of methyl H,C shifts are a result of a combination of the diamagnetic, contact and pseudocontact contributions to the chemical shifts of both nuclei,²⁴

$$\delta^H = \delta^H_{\text{dia}} + \delta^H_{\text{con}} + \delta^H_{\text{pcM}} \quad (1)$$

$$\delta^C = \delta^C_{\text{dia}} + \delta^C_{\text{con}\pi} + \delta^C_{\text{pcM}} + \delta^C_{\text{pcL}\pi} \quad (2)$$

where δ^H_{dia} and δ^C_{dia} are the shifts of the same nuclei in a diamagnetic complex (usually Zn(II)-substituted complexes are used to evaluate these^{27,39–41}), δ^H_{con} is the proton contact shift contribution, and $\delta^C_{\text{con}\pi}$ is the corresponding carbon contact shift for delocalization of the unpaired electron from the metal to the ligand through π bonds. The pseudocontact (formerly called dipolar^{39,40}) shifts, δ^H_{pcM} and δ^C_{pcM} , are the result of the through-space dipolar coupling between the nucleus of interest (H or C) and the electron, which is centered on the metal, because of the magnetic anisotropy of d-orbitals, which produce an angular and distance dependence on the size of the pseudocontact shift and can be calculated if one knows the distance and angular relationship between each nucleus and the metal center from the X-ray crystal structure.^{24,39–41} In addition, for nuclei larger than hydrogen there is an additional contribution, $\delta^C_{\text{pcL}\pi}$, which arises because of spin delocalization from the metal to the macrocycle via π bonds, and then through space to aliphatic carbons that are connected to the carbon of the π system. Wüthrich and Baumann considered all of these terms in 1973, in the first report of the natural-abundance direct-detect ^{13}C NMR spectra of synthetic and natural heme complexes,¹ but they also included potential σ contributions to the contact, metal-centered pseudocontact and ligand-centered pseudocontact shifts of the carbons, which have since been shown to be unimportant for low-spin Fe(III) complexes, where the unpaired electron is in a π -symmetry d-orbital.^{24,39–41}

The situation for low-spin Fe(III) is that the diamagnetic shifts of all protons and carbons of substituents at the heme β -pyrrole positions are similar, the metal-centered pseudocontact shifts are fairly small, and the ligand-centered pseudocontact shifts vary linearly with the contact shifts,⁴² which are large. Thus the combination of these contributions, with the dominance of the contact shifts, move these cross peaks well outside the normal ranges observed for the two nuclei in diamagnetic compounds, and thus make them easy to recognize and assign.

Thus, the approximately linear correlation is basically a result of the fact that the contact contribution dominates the chemical shifts of both protons and ^{13}C in low-spin Fe(III) compounds, at least for those present at the β -pyrrole positions. The McConnell equation relates the hyperfine coupling constants a_H and a_C , which are directly proportional to the contact shifts of each nucleus, for the β -pyrrole positions to the electron density at the β -pyrrole carbons,⁴³ and this is true for both the ^1H and the ^{13}C contact shifts:

$$a_H = Q_H \rho_C / 2S \text{ for } ^1\text{H}, \quad (3)$$

where $Q_H \sim +70\text{--}75$ MHz for methyl groups attached to sp^2 -hybridized carbons that are part of the π system,^{44,45} and

$$a_C = Q_C \rho_C / 2S \text{ for } ^{13}\text{C}, \quad (4)$$

where $Q_C \sim -39$ MHz for sp^3 -hybridized carbons that are bound to sp^2 -hybridized carbons that are part of the π system,^{18,46,47} with a ligand-centered pseudocontact shift for ^{13}C which is linearly related to the ^{13}C contact shift.^{24,42}

For systems in which there is a very small difference in chemical shifts of the pyrrole-H resonances, such as the case of the $[2\text{-ClTPPFe}(\text{CN})_2]^-$ complex³⁶ shown in Figure 2 (overall ^1H range = 1.6 ppm), the diamagnetic chemical shifts of the pyrrole-H and -C resonances, which must differ because of the substituent effect of the 2-chloro group, probably contribute to masking a clear linear correlation of the H,C cross peaks for this complex and for other $[2\text{-XTPPFe}^{\text{III}}(\text{CN})_2]^-$ where the ^1H chemical shift range is significantly larger,³⁶ because there still is not a linear correlation of the ^1H and ^{13}C chemical shifts. This is probably because of the additional contributions to the carbon diamagnetic shifts because of the substituent, and to the ligand-centered pseudocontact contributions to the paramagnetic shifts (eq. (2)).²⁴ However, for phenyl-substituted $\text{TPPFe}^{\text{III}}$ bis-imidazole complexes which have sufficiently large spreads of the β -pyrrole H and C resonances, linear correlations are observed, but with much steeper slopes, as shown in Figure 3, as will be discussed further below. We have observed these linear correlations for methyl resonances of $S = 1/2$ ferrihemin complexes, as well as for the $S = 1$ iron corrole complex shown in Figure 4, where the slope is approximately double that for a $S = 1/2$ system (Table 1).

For the His/Met-coordinated ferriheme centers of horse cytochrome *c*, cyanobacterial cytochromes c_6 and bacterial cytochrome *c*-551, the His/His-coordinated cytochromes c_3 , bis-His met-Hbs, cytochrome b_5 and the cyanide complexes of myoglobin and bacterial heme oxygenases, as well as the azide complexes of the latter, the observed slope of this line is typically -1.8 to -2.2 . This slope appears to be a hallmark of the $(d_{xy})^2(d_{xz}, d_{yz})^3$ electron (or d_{π}^1 hole) configuration of the ferriheme center, since His/Met- and His/His-coordinated ferriheme complexes invariably have this ground state. The same is true for the imidazole and histamine complexes of the nitrophorin proteins, as summarized in Table 1, although the range in the slope is somewhat larger (-1.7 to -2.3).³⁵ This larger range is undoubtedly because of the strongly nonplanar nature of the nitrophorin hemes,^{48,49} which tends to mix in some d_{xy} character.³¹ If only the contact shift of equations (1) and (2) were to contribute, then according to equations (3) and (4) the ratio $Q_C/Q_H = -0.52$ to -0.56 . When corrected for the difference in magnetogyric ratio of ^1H and ^{13}C ($Q_C\gamma_H/Q_H\gamma_C$), the ratio of $\delta^{\text{C}}_{\text{con}\pi}/\delta^{\text{H}}_{\text{con}}$ is predicted to be -2.08 to -2.24 , which is very close to what is observed for the slope of the lines for the majority of $S = 1/2$ ferriheme complexes (see Table 1).

Although the correlation and actual slopes of many of the lines are in fact between -1.8 and -2.2 , the steeper slope of the $[(o\text{-CONMe}_2)_1\text{TPPFe}(\text{NMeIm})_2]\text{Cl}$ complex (-6.85) suggests that this case of β -pyrrole carbons and their directly-bound protons behaves a different relationship than is present for methyl groups (eq. 3 and 4). This is in part due to the fact that the Q values are somewhat different in this case, but there are more differences to be considered; in fact, the much greater slope for this model complex is due to the combination of three factors: 1) the direct 1-bond relationship between the carbon of the π system and the pyrrole protons of interest,⁵⁰ 2) the substituent effect of the single *ortho*-dimethylamide on one phenyl ring,⁴⁵ and 3) the dynamics of the complex.⁵¹ The Q_C value for an sp^2 -hybridized carbon that is part of an extended π system is $+54.6$ MHz,⁵⁰ and the Q_H of a proton directly attached to this sp^2 -hybridized carbon is -65.8 MHz,⁵⁰ which together yield a predicted slope, $\delta^{\text{C}}_{\text{con}\pi}/\delta^{\text{H}}_{\text{con}}$ of -3.32 . However, instead of a slope of -3.32 , one that is approximately double that value, -6.85 , is observed. This is a result of the fact that the dimethylamide substituent on one *ortho* position of one phenyl group of the tetraphenylporphyrin provides a substituent effect that makes the chemical shifts of the pyrrole protons different from each other *and also* hinders, but does not completely prevent, the rotation of the N-methylimidazole ligand bound on that side of the heme plane.

Typically, in model heme complexes the planar axial ligands rotate extremely rapidly, on the order of hundreds of thousands to a million times per second;^{52,53} this makes model heme

complexes very different from heme proteins, where axial ligands are held in fixed orientations by the design of the protein. This rapid rotation of model heme axial ligands averages the differences in pyrrole-proton chemical shifts to the differences observed for such complexes due to the substituent effect of a unique substituent (up to 3 ppm).⁴⁵ However, the bulky dimethylamide substituent was designed to hinder the rotation of one of the N-methylimidazole ligands in order to simulate the fixed position of axial ligands in proteins. But although its rotation is slowed considerably, it is not stopped, which gives the pyrrole protons quite variable chemical shifts as the temperature is changed.⁵⁰ As shown in the lower insert of Figure 5, at low temperatures a total of 7 resolved resonances of the 8 protons are resolved, which collapse to three at the highest temperature studied in the original work at 300 MHz.⁵⁰ As the temperature is raised the slope decreases, but does not reach the predicted $\delta^C_{\text{con}\pi}/\delta^H_{\text{con}}$ of -3.32 by temperatures near the boiling point of the solvent. Hence, model heme complexes, even with bulky substituents, cannot fully simulate the major effect of the fixed orientation of one axial ligand (or both in the case of cytochromes b_5 , c , c_3 and the cyanobacterial methemoglobins) discussed above. The methyls of the bis-imidazole complex of iron(III) protoporphyrin IX,²⁵ however, where the ligands can spin very rapidly, shows a slope δ^C/δ^H only slightly larger than the expected slope, of -2.41 . This slightly larger slope is probably due to the substituent effect of the two vinyl groups, which lead to somewhat different diamagnetic shifts for the 1,3M and the 5,8M.

In contrast to the typical $\delta^C_{\text{con}\pi}/\delta^H_{\text{con}} \sim -2.0$ for the His-His, His-Met and His-cyanide-bound complexes of most proteins, for the cyanide complexes of the nitrophorins, the slope is typically -0.8 to -1.4 ,^{31,33,35} which appears to be a hallmark of the $(d_{xz}, d_{yz})^4(d_{xy})^1$ electron configuration of the ferriheme center.³¹ (There are no other ferriheme protein systems to which the nitrophorins can be compared, because most heme cyanide complexes of alpha-helical heme proteins do not have the $(d_{xz}, d_{yz})^4(d_{xy})^1$ electron configuration, or at best exhibit a mixed electronic ground state.³¹ This is because most ferriheme proteins do not have ruffled hemes; a ruffled distortion of the ferriheme has been shown to be required to stabilize the $(d_{xz}, d_{yz})^4(d_{xy})^1$ electron configuration of the ferriheme center,^{31,54,55} because only when there is a ruffling distortion of the heme does a d_{xy} unpaired electron on Fe have the proper symmetry to accept π donation from a filled π orbital on the porphyrin (the $a_{2u}(\pi)$ orbital).) In this electronic ground state, the majority of the spin density is on the *meso*-carbons, and we have not as yet detected either the proton or the carbon signals of the *meso*-carbons of the cyanide complexes of the nitrophorins. Thus, the much smaller amount of spin density present at the methyl groups of the protohemin macrocycles of these cyanide complexes is more prone to variations in the diamagnetic and metal-centered pseudocontact shifts of equations (1) and (2) than are the larger spin densities of the His/His and His/Met-coordinated heme proteins.

Comments about specific low-spin ferriheme protein systems that should be made include the following:

1. The 3M cross peak often deviates from the linear correlation, as seen in Figs. 5 – 7, but not in Figs. 1 or 8. For Fig. 1, the four hemes each have cross peaks that deviate from the best line, but while points 4, 10, 12 and 17 are the four 3M cross peaks, points 3, 7, 9 and 14 are the four 5M cross peaks and point 15 is a 1M cross peak.
2. Although we first noticed that there was a correlation between ^1H and ^{13}C shifts of methyl groups for the nitrophorins, they actually follow this correlation more poorly than do other heme proteins, probably in large part because they are significantly ruffled, and also because dynamics prevents several important cross peaks from being observed. Ruffling not only creates the $(d_{xy})^1$ ground state, but it also changes the pseudocontact shifts by reversing the sign ($g_{\parallel} < g_{\perp}$) and

decreasing the magnitude of the magnetic anisotropy to $\sim 1/4$ or less of its magnitude for the $(d_{xz}, d_{yz})^3$ ground state systems, and also causes a very slightly variable distance between Fe and the methyl groups. In that respect, 3M is in a different geometrical position with respect to the propionate groups than are 1M, 5M and 8M, and thus its chemical shifts are expected to be differently altered by nonplanarity of the heme. In addition, the effects of macrocycle ruffling on the diamagnetic shifts in the absence of the half-filled d_{xy} orbital are unknown, and may well be variable. The histamine and imidazole complexes tend to follow a linear correlation better than do the cyanide complexes, in line with the fact that the cyanide complexes are the most nonplanar and have a large degree of $(d_{xy})^1$ character to the orbital of the unpaired electron.³¹

3. Although the plots for the bacterial heme oxygenase-cyanide (HO-CN) complexes are more linear than those of the cytochromes b_5 , c and the nitrophorins, the corresponding azide complexes (HO-N₃) have smaller ¹³C shifts as compared to the others, which appears to make the azide complexes stand out as different from the cyanide complexes. This adds strength to the conclusion that the spin state for the azide complexes is not the same as that of the cyanide complexes; the authors had concluded that the azide complexes had a major contribution from an $S = 3/2$ spin state species.¹³

Acknowledgments

The support of the National Institutes of Health, grant DK031038, is gratefully acknowledged. This paper was written while FAW was a visiting professor at the Institute for Molecular and Cell Biology at Rosario, Santa Fe, Argentina, and she thanks Prof. Alejandro J. Vila for his hospitality.

References

1. Wuthrich K, Baumann R. *Biochim Biophys Acta*. 1973; 56:585–596.
2. Goff H. *Biochim Biophys Acta*. 1978; 542:348–355. [PubMed: 687661]
3. Goff HM, Shimomura ET, Phillippi MA. *Inorg Chem*. 1983; 22:66–71.
4. Goff HM. *J Am Chem Soc*. 1981; 103:3714–3722.
5. Rivera M, Walker FA. *Anal Biochem*. 1995; 230:295–302. [PubMed: 7503421]
6. Rodríguez-Marañón MJ, Qiu F, Stark RE, White SP, Zhang X, Stephen I, Foundling SI, Rodríguez V, Schilling CL III, Bunce RA, Rivera M. *Biochemistry*. 1996; 35:16378–16390. [PubMed: 8973214]
7. Bunce RA, Schilling CL III, Rivera M. *J Labelled Compd and Radiopharm*. 1997; 39:669–675.
8. Qiu F, Stark RE, Rivera M. *NMR Newsletter*. 1996:5–6.
9. Qiu F, Rivera M, Stark RE. *J Magn Reson*. 1998; 130:76–81. [PubMed: 9469900]
10. Rivera M, Qiu F, Bunce RA, Stark RE. *J Biol Inorg Chem*. 1999; 4:87–98. [PubMed: 10499106]
11. Caignan GA, Deshmukh R, Wilks A, Zeng Y, Huang H, Moënné-Loccoz P, Bunce RA, Eastman MA, Rivera M. *J Am Chem Soc*. 2002; 124:14879–14892. [PubMed: 12475329]
12. Zeng Y, Deshmukh R, Caignan GA, Bunce RA, Rivera M, Wilks A. *Biochemistry*. 2004; 43:5222–5238. [PubMed: 15122888]
13. Zeng Y, Caignan GA, Bunce RA, Rodriguez JC, Wilks A, Rivera M. *J Am Chem Soc*. 2005; 127:9794–9807. [PubMed: 15998084]
14. Wegele R, Tasler R, Zeng Y, Rivera M, Frankenberg-Dinkel N. *J Biol Chem*. 2004; 279:45791–45802. [PubMed: 15310749]
15. Deshmukh R, Zeng Y, Furci LM, Huang H, Morgan BN, Sander S, Alontaga AY, Bunce RA, Moënné-Loccoz P, Rivera M, Wilks A. *Biochemistry*. 2005; 44:13713–13723. [PubMed: 16229461]
16. Santos H, Turner DL. *FEBS Lett*. 1986; 194:73–77. [PubMed: 3000825]

17. Turner DL, Salgueiro CA, Schenkels P, LeGall J, Xavier AV. *Biochim Biophys Acta*. 1995; 1246:24–28. [PubMed: 7811726]
18. Turner DL. *Eur J Biochem*. 1995; 227:829–837. [PubMed: 7867644]
19. Costa HS, Santos H, Turner DL. *Eur Biophys J*. 1996; 25:19–24.
20. Brennan L, Turner DL. *Biochim Biophys Acta*. 1997; 1342:1–12. [PubMed: 9366264]
21. Salgueiro CA, Turner DL, Xavier AV. *Eur J Biochem*. 1997; 244:721–734. [PubMed: 9108240]
22. Louro RO, Medina M, Aguiar AP, Hervás M, De la Rosa M, Gómez-Moreno C, Turner DL, Xavier A. *J Biol Inorg Chem*. 1998; 3:68–73.
23. Louro RO, Correia IJ, Brennan L, Coutinho IB, Xavier AV, Turner DL. *J Am Chem Soc*. 1998; 120:13240–13247.
24. Timkovich R. *Inorg Chem*. 1991; 30:37–42.
25. Banci L, Bertini I, Pierattelli R, Vila AJ. *Inorg Chem*. 1994; 33:4338–4343.
26. Banci L, Bertini I, Luchinat C, Pierattelli R, Shokhirev NV, Walker FA. *J Am Chem Soc*. 1998; 120:8472–8479.
27. Hu B, Hauksson JB, Tran A-T, Kolczak U, Pandey RK, Rezzano IN, Smith KM, La Mar GN. *J Am Chem Soc*. 2001; 123:10063–10070. [PubMed: 11592885]
28. Vu BC, Vuletich DA, Kuriakose SA, Falzone CJ, Lecomte JTJ. *J Biol Inorg Chem*. 2004; 9:183–194. [PubMed: 14727166]
29. Shokhireva TK, Shokhirev NV, Walker FA. *Biochemistry*. 2003; 42:679–693. [PubMed: 12534280]
30. Shokhireva TK, Berry RE, Uno E, Balfour CA, Zhang H, Walker FA. *Proc Natl Acad Sci USA*. 2003; 100:3778–3783. [PubMed: 12642672]
31. Shokhireva TK, Weichsel A, Smith KM, Berry RE, Shokhirev NV, Balfour C, Zhang H, Montfort WR, Walker FA. *Inorg Chem*. 2007; 46:2041–2056. [PubMed: 17290983]
32. Shokhireva TK, Shokhirev NV, Berry RE, Zhang H, Walker FA. *J Biol Inorg Chem*. 2008; 13:941–959. [PubMed: 18458965]
33. Shokhireva TK, Berry RE, Zhang H, Shokhirev NV, Walker FA. *Inorg Chim Acta*. 2008; 361:925–940.
34. Yang F, Zhang H, Knipp M. *Biochemistry*. 2009; 48:235–241. [PubMed: 19140692]
35. Yang F, Knipp M, Berry RE, Shokhireva TK, Zhang H, Walker FA. *J Biol Inorg Chem*. 2009; 14:1077–1095. [PubMed: 19517143]
36. Wojaczynski J, Latos-Grazynski L, Hrycyk W, Pacholska E, Rachlewicz K, Szterenberg L. *Inorg Chem*. 1996; 35:6861–6872. [PubMed: 11666854]
37. Nardis S, Paolessee R, Licoccia S, Fronczek FR, Vicente MGH, Shokhireva TK, Walker FA. *Inorg Chem*. 2005; 44:7030–7046. [PubMed: 16180865]
38. Shokhirev NV, Walker FA. *J Biol Inorg Chem*. 1998; 3:581–594.
39. La Mar, GN.; Walker, FA. *The Porphyrins*. Dolphin, D., editor. Vol. IV. Academic Press; N.Y: 1979. p. 61-157.
40. Walker, FA. *The Porphyrin Handbook*. Kadish, KM.; Smith, KM.; Guillard, R., editors. Vol. Chapter 36. Academic Press; Boston: 2000. p. 81-183.
41. Walker, FA. *Handbook of Porphyrin Science*. Kadish, KM.; Smith, KM.; Guillard, R., editors. Vol. VI. World Scientific; Hackensack NJ: 2010. p. 1-337. Chapter 29
42. Unger SW, Jue T, La Mar GN. *J Magn Reson*. 1985; 61:448–456.
43. McConnell HM. *J Chem Phys*. 1956; 24:764–766.
44. Derbyshire W. *Mol Phys*. 1962; 5:225–231.
45. Tan H, Simonis U, Shokhirev NV, Walker FA. *J Am Chem Soc*. 1994; 116:5784–5790.
46. Turner DL. *Eur J Biochem*. 1993; 211:563–568. [PubMed: 8382155]
47. Bolton JR, Fraenkel GK. *J Chem Phys*. 1964; 40:3307–3320.
48. Walker FA. *J Inorg Biochem*. 2005; 99:216–236. [PubMed: 15598503]
49. Walker, FA. *The Smallest Biomolecules: Diatomics and their Interactions with Heme Proteins*. Ghosh, A., editor. Elsevier B. V; 2008. p. 378-428.

50. Bertini, I.; Luchinat, C. NMR of Paramagnetic Substances. In: Lever, ABP., editor. *Coord Chem Rev.* Vol. 150. 1996. p. 29-75.table 2.7
51. Zhang H, Simonis U, Walker FA. *J Am Chem Soc.* 1990; 112:6124–6126.
52. Shokhirev NV, Shokhireva TKh, Polam JR, Watson CT, Raffii K, Simonis U, Walker FA. *J Phys Chem A.* 1997; 101:2778–2886.
53. Polam JR, Shokhireva TKh, Raffii K, Simonis U, Walker FA. *Inorg Chim Acta.* 1997; 263/1–2:109–117.
54. Safo MK, Walker FA, Raitsimring AM, Walters WP, Dolata DP, Debrunner PG, Scheidt WR. *J Am Chem Soc.* 1994; 116:7760–7770.
55. Walker FA. *J Inorg Biochem.* 2005; 99:216–236. [PubMed: 15598503]

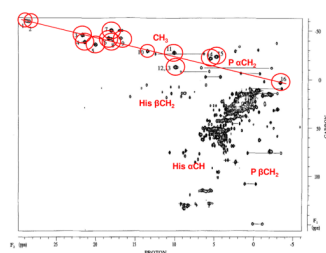


Figure 1.

HMQC spectrum of the bis-histidine-coordinated tetraheme protein from *Desulfovibrio vulgaris*, cytochrome *c*₃ (Hildenborough) at 38.3 °C and pH 9.0. The heme methyls of the four hemes in the protein are labeled **1 – 16**. A number of other resonances have been assigned, including most of the propionate α-CH₂, some of the β-CH₂, the His α-CH and β-CH₂ resonances.²¹ $\delta_C/\delta_H = -2$. Modified from Ref. ²¹ with permission from the Federation of European Biochemical Societies.

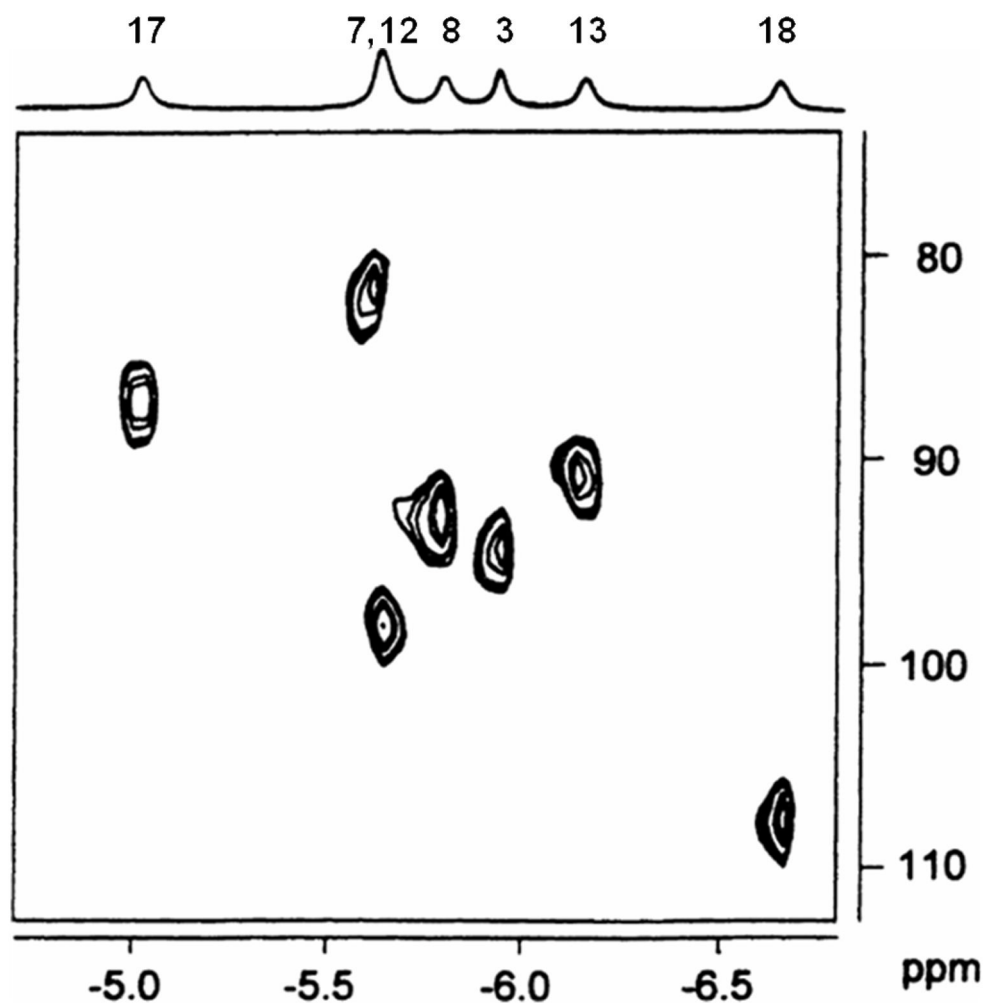


Figure 2.

The pyrrole region of the 300 MHz ^1H - ^{13}C HMQC spectrum of $[(2\text{-Cl-TPP})\text{Fe}^{\text{III}}(\text{CN})_2]^-$ in methanol- d_4 at 294 K. There is no $\delta_{\text{C}}/\delta_{\text{H}}$ correlation observed, probably because of the extremely small range of δ_{C} and δ_{H} observed, which magnifies the importance of the differences in diamagnetic shifts. Modified from Reference ¹⁸ with permission from the American Chemical Society.

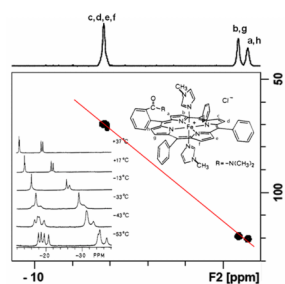


Figure 3.

HMQC spectrum of the pyrrole-H region of $[(o\text{-CONMe}_2)^1\text{TPPFe}(\text{NMIm})_2]^+$, recorded at 500 MHz in CDCl_3 at 25 °C. Upper insert shows the structure of the complex and the eight types of pyrrole protons present (a – h). Lower insert shows the published temperature dependence of the spectra, recorded earlier, at 300 MHz.⁵¹ Reprinted from Fei Yang, unpublished, with her permission.

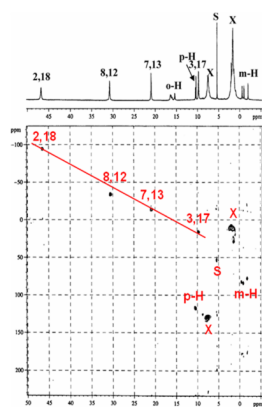


Figure 4. 1D ^1H and 2D $^1\text{H}\{^{13}\text{C}\}$ -HMQC spectra of chloroiron(III) octamethyltriphenylcorrolate, (OMTPCorr)FeCl. The ^1H - ^{13}C correlations for the four methyl, two *para*-phenyl, and four *meta*-phenyl groups are shown; the relaxation times of the *ortho*-phenyl protons are too short to allow their correlations to be detected. Resonances marked X are those of corrole decomposition products. Recorded in CD_2Cl_2 at 25 $^\circ\text{C}$ and 500 MHz. Least squares $\delta_{\text{C}}/\delta_{\text{H}} = -3.17$. Modified from Ref. ³⁷ with permission of the American Chemical Society.

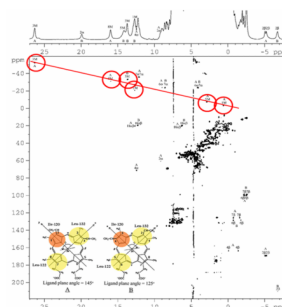


Figure 5. 1D and ^1H - ^{13}C HMQC NMR spectra of NP2(V24E)-ImH in D_2O , buffered with 30 mM $\text{Na}_2\text{DPO}_4/\text{acetic acid-}d_4$ ($\text{pH}^* 7.0$), recorded at 35 $^\circ\text{C}$, 500 MHz. There are two sets cross peaks, one from isomer **A**, and the other from isomer **B**. The 5M isomer **B** ^1H resonance is broadened because of some sort of chemical exchange, and it does not give a ^1H , ^{13}C cross peak. The **A** and **B** heme orientations are shown in the insert. Modified from Reference ³⁵ with permission from Elsevier Publishing Company.

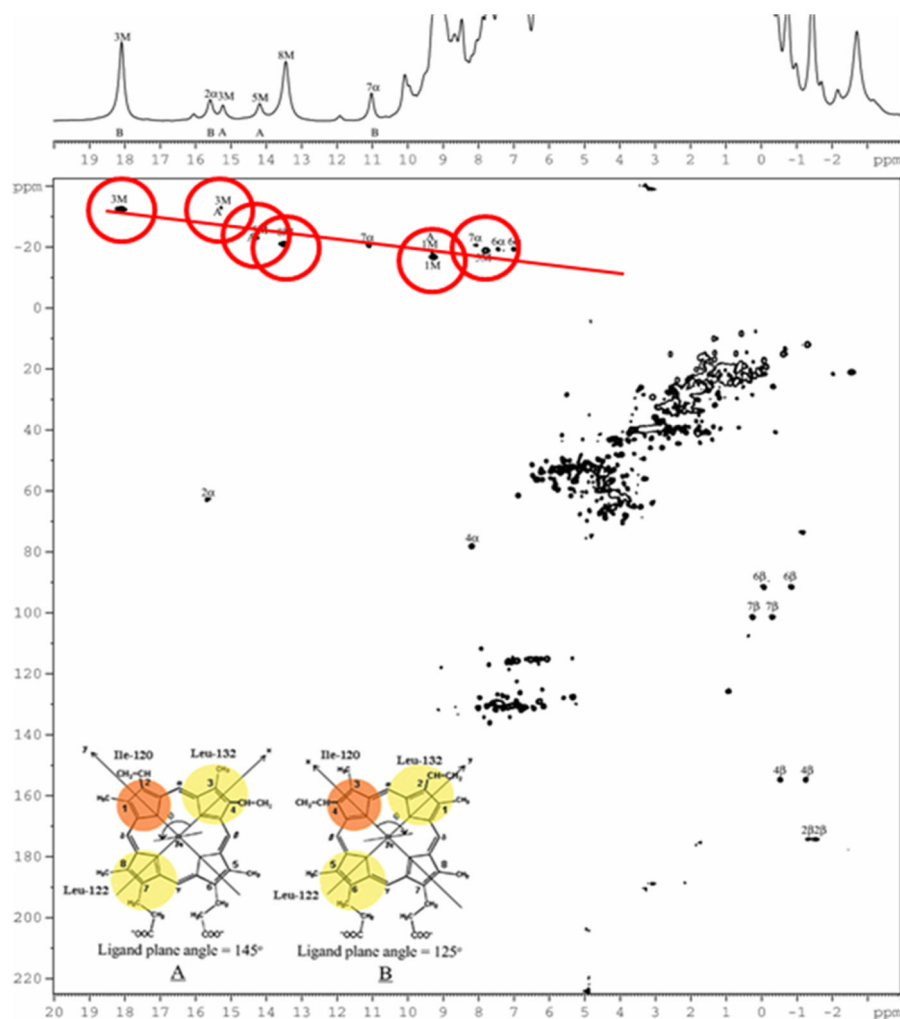


Figure 6. 1D and ^1H - ^{13}C HMQC spectra of NP2-CN in D_2O , buffered with 30 mM $\text{Na}_2\text{DPO}_4/\text{acetic acid-}d_4$ ($\text{pH}^* 6.5$), recorded at 35 °C and 500 MHz. The **A** and **B** heme orientations are shown in the insert. Modified from Reference ³⁵ with permission from Elsevier Publishing Company.

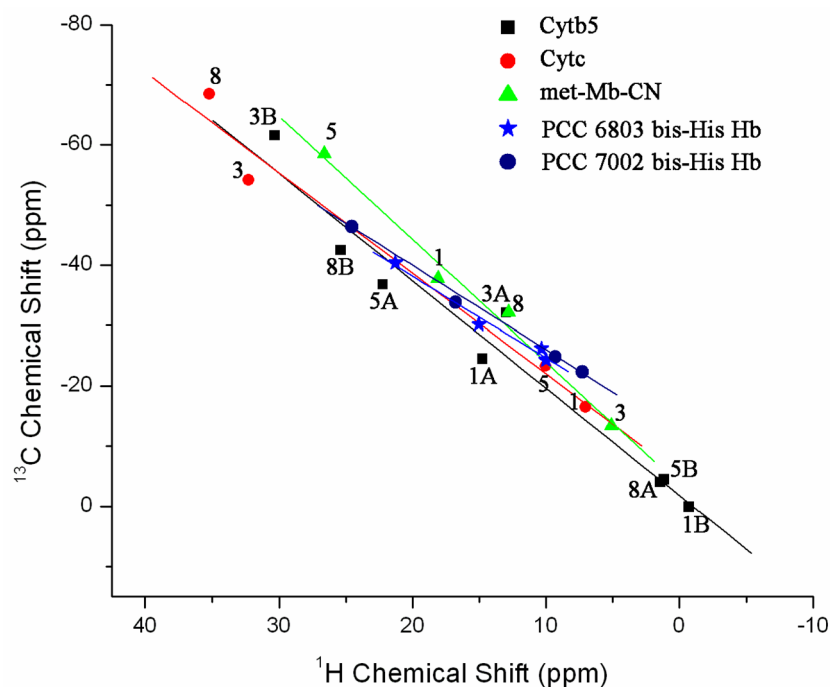


Figure 7. Plot of ^{13}C vs. ^1H chemical shifts for horse cytochrome c ,²⁴ rat OM cytochrome b_5 ,¹⁰ met-Mb-CN²⁷ and two cyanobacterial 6-coordinate (bis-His) met-Hbs.²⁸ Note that in the first three cases the 3-methyl points deviate from the best fit line. Including 3M, for cyt c $\delta_{\text{C}}/\delta_{\text{H}} = -1.67$; without 3M it is -1.82 ; for met-Mb-CN $\delta_{\text{C}}/\delta_{\text{H}} = -2.04$ with 3M, $\delta_{\text{C}}/\delta_{\text{H}} = -1.9$ without 3M. Including 3MA and 3MB for OM b_5 $\delta_{\text{C}}/\delta_{\text{H}} = -1.78$; without 3MA and 3MB it is -1.59 . For the cyanobacterial 6-coordinate met-Hbs 3M does not deviate from the line.

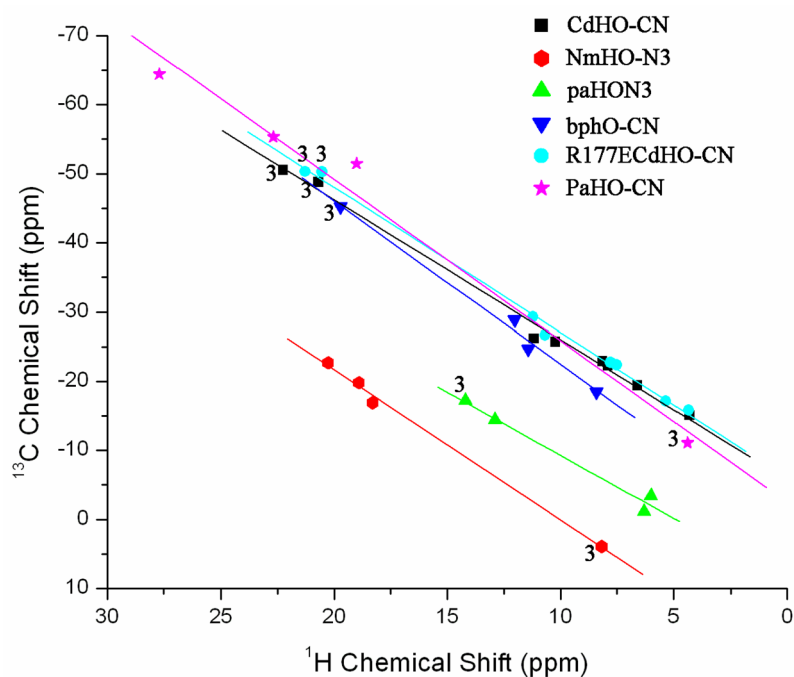


Figure 8. Plot of ^{13}C vs. ^1H chemical shifts for several bacterial heme oxygenases as the cyanide and azide complexes. Note that the 3-methyl points do not appear to deviate from the best fit lines.

Table 1

^1H and ^{13}C Chemical shifts of the heme methyls and best slopes $\delta_{\text{C}}/\delta_{\text{H}}$ for a number of ferriheme proteins.

Protein	Temp., pH °C	Heme	L_1/L_2	^1H chemical shifts, ppm				^{13}C chemical shifts, ppm				$\delta_{\text{C}}/\delta_{\text{H}}$ w, w/o 3M	Ref.
				1M	3M	5M	8M	1M	3M	5M	8M		
<i>D. vulgaris</i> cyt. c	38.3, 9.0	I	His/His	18.35	9.72	18.01	28.44	-42.32	-12.14	-50.28	-59.97	-1.98	21
		II		4.69	21.23	5.58	21.81	-23.10	-38.27	-21.50	-45.85		
		III		13.47	9.91	20.04	-3.44	-29.09	-26.99	-35.80	3.39		
		IV		17.64	9.72	16.65	28.92	-40.52	-12.14	-42.15	-60.63		
<i>S. frigidimarina</i> cyt c	35.7, 6.1	I	His/His	9.25	18.54	11.70	36.29	-22.4	-21.6	-29.7	-68.0	-1.68, -1.53	
		II		14.66	12.21	23.57	21.6	-35.4	-22.3	-51.4	-45.7		
		III		17.19	9.88	18.72	37.09	-34.6	-11.4	-47.1	-66.5		
		IV		7.37	23.11	10.96	32.00	-23.1	-44.8	-32.7	-61.9		
Horse cyt c	50, 6.7		His/Met	7.65	30.10	10.84	32.43	-16.6	-49.4	-22.8	-63.0	-1.66, -1.83	16
Horse cyt c	30, 5.3		His/Met	7.09	31.88	10.16	34.46	-17.62	-54.44	-24.06	-67.92	-1.67, -1.83	18
Horse cyt c	25, 7.0		His/Met	7.04	32.29	10.03	35.23	-16.5	-54.2	-23.3	-68.5	-1.67, -1.82	24
<i>Anabena</i> sp. cyt c ₆	34, 4.3		His/Met	15.40	35.99	21.10	38.02	-22.3	-48.3	-28.8	-59.7	-1.52, -1.69	22
<i>M. braunii</i> cyt c ₆	34, 5.5		His/Met	13.83	35.00	17.42	37.10	-20.9	-49.5	-26.0	-61.2	-1.58, -1.75	22
<i>Px. aeruginosa</i> cyt c-551	32, 7		His/Met	24.80	13.47	31.25	17.17	-46.9	-21.8	-54.3	-35.9	-1.76, -1.31	24
Horse cyt c-CN	44, 6.9		His/CN ⁻	15.46	11.46	21.29	20.79	-37.55	-20.37	-44.47	-49.77	-2.60, -1.64	20
metMb-CN	RT, 7.4		His/CN ⁻	18.3	4.8	26.4	12.5	-38.4	-14.2	-58.2	-32.0	-2.04	25
metMb-CN	RT, ~7.5		His/CN ⁻	18.1	5.1	26.6	12.8	-37.8	-13.4	-58.5	-32.2	-2.04	27
<i>Synechocystis</i> sp. PCC 6803 bis-His Hb	25, 7		His/His	15.03	9.99	21.28	10.33	-30.2	-24.3	-40.4	-26.2	-1.6	28
<i>Synechococcus</i> sp. PCC 7002 bis-His Hb	25, 7		His/His	16.77	7.28	24.55	9.30	-33.8	-22.3	-46.4	-24.8	-1.6	28
Rat OM cyt b ₅	RT, 7.0	A	His/His	14.75	12.99	22.23	1.43	-24.5	-32.1	-36.8	-4.0	-1.78, -1.59	10
		B		-0.71	30.33	1.16	25.38	0.1	-61.6	-4.5	-42.5		
<i>Px. aerug.</i> HO-CN	10, 7.4		His/CN ⁻	22.69	4.41	27.71	19.01	-55.32	-11.10	-64.44	-51.45	-2.33	11
<i>C. diphth.</i> HO-CN	10, 7.4	A	His/CN ⁻	4.32	20.69	7.91	10.23	-15.12	-48.82	-22.28	-25.67	-2.02, -1.66	12
		B		6.60	22.26	8.15	11.17	-19.41	-50.46	-22.94	-26.18		

Protein	Temp., pH °C	Heme	L ₁ /L ₂	¹ H chemical shifts, ppm				¹³ C chemical shifts, ppm				δ_C/δ_H w, w/o 3M	Ref.
				1M	3M	5M	8M	1M	3M	5M	8M		
<i>C. diphth.</i> HO R177E-CN	10, 7.4	A	His/CN ⁻	4.36	20.55	7.52	11.21	-15.82	-50.26	-22.41	-29.30	-2.10	12
				5.34	21.29	7.78	10.68	-17.15	-50.32	-22.73	-26.69		
				19.94	6.05	27.47	22.81	-45.41	-15.77	-60.14	-53.87		
bphO-CN	30, 7.0		His/CN ⁻	8.41	19.73	11.42	12.03	-18.43	-45.17	-24.64	-28.91	-2.36	14
<i>N. meningitidis</i> HO-N ₃	25, 7.0		His/N ₃ ⁻	18.90	8.17	18.31	20.26	-19.77	3.90	-16.91	-22.70	-2.17	13
<i>Ps. aeruginosa</i> HO-N ₃	25, 7.0		His/N ₃ ⁻	6.29	14.15	5.96	12.91	-1.12	-17.21	-3.40	-14.38	-1.82	13
NP2-Hm	35, 5.5	A	His/Hm	-1.5	30.4	~10.4	16.0	-2.7	-63.6	----	-32.0	-1.87	35
NP2(V24E)-ImH	35, 7.0	A	His/ImH	14.6	15.0	15.3	0.2	-24.1	-36.8	-30.5	-5.4		
				0.6	26.4	2.9	16.0	-3.4	-52.5	-7.4	-31.1	-1.90	35
NP1-Hm	20, 7.0	A	His/Hm	12.8	13.8	14.2	2.5	-20.8	-33.2	----	----		
				-1.3	29.3	13.7	13.8	-1.6	-64.1	-27.0	-39.1	-2.03	31
NP1-CN	20, 7.0	A	His/CN ⁻	12.9	13.9	13.4	39.1	-21.8	-39.1	-28.2	-5.4		
				10.8	16.5	13.4	7.3	-22.7	----	-27.9	-21.3	-1.15	31
NP4-CN	20, 7.0	A	His/CN ⁻	8.2	19.8	7.3	12.9	-18.8	----	-21.3	-26.8		
				10.2	16.9	12.9	7.7	-22.2	----	-27.6	-22.8	-1.07	31
NP2-CN	30, 7.0	A	His/CN ⁻	8.6	19.4	7.9	12.5	-19.5	----	-22.3	-26.2		
				9.3	15.8	14.2	7.9	-18.2	-34.9	-20.5	-20.2	-1.28, -0.62	31
Fe ^{III} ppIX(ImH) ₂	RT, DMSO	B	ImH/ImH	7.9	18.4	7.8	13.4	-19.6	-34.6	-20.2	----		
				14.1	11.8	18.0	18.4	-32.1	-26.3	-41.4	-42.0	-2.41	25
[(o-CONMe ₂) ₁ TPPFe(NMeIm) ₂] ¹⁺	25, CDCl ₃			-13.6	-13.6	-20.7	-21.3	72	72	119	120	-6.85	<i>a</i>
[OMTPCorrFeCl]	25, CD ₂ Cl ₂			46.4	9.7	20.9	30.6	-93.3	+17.4	-12.5	-32.7	-3.17	37

^aYang, F. Unpublished.